Analysis of Reaction-Diffusion Systems with Anomalous Subdiffusion

Jason M. Haugh*
Department of Chemical and Biomolecular Engineering, North Carolina State University, Raleigh, North Carolina

ABSTRACT Reaction-diffusion equations are the cornerstone of modeling biochemical systems with spatial gradients, which are relevant to biological processes such as signal transduction. Implicit in the formulation of these equations is the assumption of Fick's law, which states that the local diffusive flux of species *i* is proportional to its concentration gradient; however, in the context of complex fluids such as cytoplasm and cell membranes, the use of Fick's law is based on empiricism, whereas evidence has been mounting that such media foster anomalous subdiffusion (with mean-squared displacement increasing less than linearly with time) over certain length scales. Particularly when modeling diffusion-controlled reactions and other systems where the spatial domain is considered semi-infinite, assuming Fickian diffusion might not be appropriate. In this article, two simple, conceptually extreme models of anomalous subdiffusion are used in the framework of Green's functions to demonstrate the solution of four reaction-diffusion problems that are well known in the biophysical context of signal transduction: fluorescence recovery after photobleaching, the Smolochowski limit for diffusion-controlled reactions in solution, the spatial range of a diffusing molecule with finite lifetime, and the collision coupling mechanism of diffusion-controlled reactions in two dimensions. In each case, there are only subtle differences between the two subdiffusion models, suggesting how measurements of mean-squared displacement versus time might generally inform models of reactive systems with partial diffusion control.

INTRODUCTION

Cell cytoplasm is crowded and chemically diverse, properties that no doubt influence molecular interactions in ways that are as yet poorly characterized. Molecular diffusion, along with forced convection and active transport in some contexts, allows intracellular molecules to encounter one another, and it is therefore fundamental to interactions and biochemical conversions in metabolic and signal transduction pathways (1). The influence of molecular crowding is acute in cellular membranes; it has long been appreciated that the plasma membrane is organized into dynamic subcompartments (2). Even in the bulk, disordered plasma membrane, single-molecule imaging has revealed complex molecular mobility dynamics consistent with ''hop'' diffusion across corral-like barriers with a characteristic spatial dimension of ~100 nm (3). These complex transport phenomena have not yet been taken into account in biophysical models of biochemical reaction networks in cells (4).

Generally speaking, any macroscopic reaction-transport system that is modeled as a continuum is comprised of conservation equations, with their associated initial and boundary conditions, and constitutive equations. The conservation of a particular molecular species *i* is expressed in terms of its concentration, C_i, as follows (5):

$$\frac{\partial C_i}{\partial t} = -\nabla \cdot \mathbf{N}_i + R_i. \quad (1)$$

This bookkeeping equation is applicable to transport in 1, 2, or 3 dimensions; throughout this article, the dimensionality is defined as *n*, and C_i is the density of species *i* per unit length^n. The accumulation of species *i* at a particular location and time, *t*, has two contributions: net molecular transport and chemical reaction. The first of these establishes the definition of the species *i* flux vector, $\mathbf{N}_i$, which accounts for both convection (drift) and diffusion (dispersion) of species *i*. In the context of our model, we consider diffusive transport only; in the commonly used notation, $\mathbf{N}_i = \mathbf{J}_i$. Finally, the source term R_i is the overall rate of species *i* formation by chemical reaction.

To proceed further, a constitutive equation must be specified that relates the diffusive portion of the flux $\mathbf{J}_i$ to C_i and other measurable properties of the transport medium. The standard approach is to invoke Fick's law, with the implicit assumption of a dilute (at least with respect to species *i*), isotropic medium:

$$\mathbf{J}_{r,i} = -D\frac{\partial C_i}{\partial r}. \quad (2)$$

The lone spatial variable *r* is the distance from some reference point (the initial location of a molecule, for example), and the proportionality coefficient *D* is identified as the molecular diffusivity of species *i*, which relates the length- and timescales associated with diffusion. Substituting Eq. 2 into Eq. 1 produces the reaction-diffusion equations, which almost invariably serve as the starting point for spatially extended models. This is more of a leap of faith than one might appreciate. Fick's law was derived from empirical observations, and it has been argued that its foundations are dubious for biological systems in particular (6).

Indeed, single-particle/molecule tracking and fluorescence correlation spectroscopy measurements support the notion that, at least microscopically, diffusion within and on the surface of cells is often non-Fickian. At least over certain length scales, the mean-squared displacement (MSD) of

Submitted March 5, 2009, and accepted for publication May 8, 2009.

*Correspondence: jason_haugh@ncsu.edu

Editor: Elliot L. Elson.

0006-3495/09/07/0435/8 $2.00

doi: 10.1016/j.bpj.2009.05.014

a diffusing particle as a function of time t is typically found to be a good fit to the empirical equation

$$\langle r^2 \rangle = \gamma t^{\alpha}. \quad (3)$$

The exponent α defines the linearity of the MSD with respect to time, and the parameter γ is a phenomenological proportionality constant (the typical notation for this parameter, Γ, is avoided here, because the gamma function will be invoked later on). Anomalous subdiffusion refers to systems where $\alpha < 1$. This property has been broadly attributed to cytoplasm and cell membranes (7–9), yet its origins and ubiquity remain unclear (10). Anomalous subdiffusion in cells is plausible given the complexity of cytoplasm and, in the context of the plasma membrane, the presence of lipid microdomains and/or corral-like structures (3,11,12) that serve to constrain molecular diffusion. Fick's law, of course, dictates that the MSD is proportional to time ($\alpha = 1$).

In the realm of biophysics, some attempts to account for anomalous diffusion start with Eq. 2 but allow D to vary with time (see Wu and Berland (13) and references therein); with this assumption, D needs to be proportional to $t^{\alpha-1}$ to recover Eq. 3. Conceptually, this time-dependent diffusion (TDD) model is consistent with the dissolution of otherwise closed microstructural features (cages or corrals) over a certain timescale. A distinct model of anomalous subdiffusion might be based instead on a spatial dependence on molecular mobility, with structurally stable but ''leaky'' corrals; conceptually, this length-dependent diffusion (LDD) model is consistent with the explanation of hierarchical ''hop'' diffusion in the plasma membrane (3). Hybrids of these two conceptual models are certainly plausible. Another modeling approach, not explored here, is the use of fractional diffusion equations, wherein anomalous sub- and superdiffusion are consistent with fractional derivatives in time and space, respectively (14). Such equations are equivalent, in the continuum limit, with a continuous time random walk with power-law waiting time distribution (15).

In this short article, LDD and TDD models of anomalous subdiffusion are used within the framework of Green's functions to solve four biophysically relevant reaction-diffusion problems on the infinite spatial domain. In each case, comparison of the LDD and TDD models reveals only subtle differences, which are probably not discernible by experiment.

METHODS

Formulation of the microscopic diffusion problem: length-dependent versus time-dependent diffusion

To relate diffusion behavior to the measured MSD versus time, as in Eq. 3, a microscopic description of non-Fickian diffusion needs to be invoked. For a laterally mobile molecule diffusing in n dimensions, we seek the probability density function (PDF), $p_n(r,t)$, associated with finding the molecule a distance r away from its initial position. For LDD, it is proposed that the PDF should satisfy the differential equation

$$\frac{\partial p_n(r,t)}{\partial t} = \frac{\Lambda}{r^{n-1}} \frac{\partial}{\partial r}\left[r^{n-1} \phi(r) \frac{\partial p_n(r,t)}{\partial r} \right]. \quad (4)$$

The parameter Λ is a proportionality constant; for Fickian diffusion, $\Lambda = D$ and $\phi(r) = 1$. Because r here is measured relative to each molecule's initial position, and not to fixed coordinates, Eq. 4 is conceptually distinct from the situation where Fick's law is assumed with position-dependent diffusivity, $D(\mathbf{r})$. By the same token, Eq. 4 is, by itself, insufficient for solving macroscopic diffusion problems. The solution to Eq. 4 is subject to the constraints

$$p_n(r,0) = \delta(r) \text{ and } \left.\frac{\partial p_n(r,t)}{\partial r}\right|_{r=0} = 0. \quad (5)$$

By convention, $p_n(r,t)$ is normalized according to

$$2A_n \int_0^{\infty} p_n(r,t) r^{n-1} dr = 1, \quad (6)$$

where $A_1 = 1$, $A_2 = \pi$, and $A_3 = 2\pi$.

Various semiempirical models, $\phi(r)$, might be proposed to account for non-Fickian diffusion. For example,

$$\phi(r) = r^{-\beta}; \quad (7)$$

$$\phi(r) = 1 + [\lambda_1/(\lambda_2 + r)]^{\beta}. \quad (8)$$

The latter might be more suitable if, although anomalous diffusion is observed at intermediate length scales, Fickian diffusion is apparent over larger or/and smaller length scales relevant to the problem of interest (16,17); however, we will restrict our attention to the form given in Eq. 7 because of its mathematical properties.

By comparison to results originally derived for diffusion on fractal surfaces (18), it is established that the PDF associated with Eq. 7 produces precisely the MSD behavior given by Eq. 3, with

$$\alpha = 2/(2 + \beta); \quad (9)$$

$$p_n(r,t) = \frac{\alpha^{n\alpha-1} \exp\left(-\alpha^2 r^{2/\alpha}/4\Lambda t\right)}{A_n \Gamma(n\alpha/2)(4\Lambda t)^{n\alpha/2}}, \quad (10)$$

where $\Gamma(x)$ is the gamma function (19). If the diffusing molecule is consumed by a first-order reaction with rate constant k_1, then the corresponding PDF is modified by the factor $\exp(-k_1 t)$. Because the definition of Λ is particular to the model given by Eqs. 4–7, expressing results derived from Eq. 10 in terms of Λ does not facilitate comparisons to other models; this is addressed by relating Λ to the experimental observable, γ, for this particular PDF (18):

$$\gamma = \frac{\Gamma[(n+2)\alpha/2]}{\Gamma(n\alpha/2)} \left(\frac{4\Lambda}{\alpha^2}\right)^{\alpha}. \quad (11)$$

Equation 10 is distinct from the propagator based on TDD (13,20); with $D(t) = (\alpha/2n)\gamma t^{\alpha-1}$, that propagator is as follows (13):

$$p_n(r,t) = (n/2\pi\gamma t^{\alpha})^{n/2} \exp\left(-nr^2/2\gamma t^{\alpha}\right). \quad (12)$$

The main results of this study are derived or calculated using both Eqs. 10 and 12 and then are compared in terms of the common observables γ and α.

Solution of macroscopic problems using Green's functions

The Green's function approach is to be used to solve boundary value problems in the infinite domain. Given a position vector $\mathbf{r}$, the Green's function is related to the PDF derived for the microscopic problem as follows:

$$G_n(\mathbf{r},t|\mathbf{r}') = p_n(|\mathbf{r}-\mathbf{r}'|,t). \quad (13)$$

For the examples explored here, our attention is restricted to the PDFs presented in Eqs. 10 and 12, which are applicable to anomalous diffusion with constant time exponent α.

Numerical methods

Where necessary, solutions were obtained by numerical integration (quadrature); subroutines were coded in Fortran 90 for this purpose. Solutions were benchmarked against known solutions for Fickian diffusion and by checking that the output was insensitive to changes in integration step sizes.

RESULTS AND DISCUSSION

Fluorescence recovery after photobleaching (FRAP)

We begin with an analysis of FRAP experiments because of their relevance for studying molecular diffusion in and on the surface of cells (21,22); application of FRAP to systems with anomalous diffusion, in the context of TDD, has been explored (20,23,24). To simplify matters, binding/reaction terms are not considered here. With the typical assumption of a cylindrically symmetric bleach profile, the evolution of the bleached profile $C_b(\mathbf{r},t)$ is evaluated by integration; according to the Green's function approach, the appropriate integral for polar coordinates is (5)

$$C_b(\mathbf{r},t) = 2\int_0^{\pi}\int_0^{\infty} C_b(\mathbf{r}',0)G_2(\mathbf{r},t|\mathbf{r}')r'dr'd\theta;$$
$$|\mathbf{r}-\mathbf{r}'| = \left(r^2 + r'^2 - 2rr'\cos\theta\right)^{1/2}. \quad (14)$$

The factor of 2 arises from the symmetry of the integral over θ. Here, we consider a uniform, circular bleach profile, $C_b(r,0) = 1$ (arbitrary scaling) for $r < R$ and $C_b(r,0) = 0$ for $r > R$, which is applicable to uniform light sources and a reasonable approximation for Gaussian beams with intense bleaching (21). The fractional recovery, $f(t)$, is defined as

$$f(t) = 1 - \frac{2}{R^2}\int_0^R C_b(r,t)rdr. \quad (15)$$

For the case of uniform circular bleach and Fickian diffusion, Soumpasis (25) obtained the analytical result

$$f(t) = \exp\left(-\frac{R^2}{2Dt}\right)\left[I_0\left(\frac{R^2}{2Dt}\right) + I_1\left(\frac{R^2}{2Dt}\right)\right], \quad (16)$$

where $I_0(x)$ and $I_1(x)$ are modified Bessel functions of the first kind (19).

Results were obtained by numerical integration for both the LDD (Eq. 10) and TDD (Eq. 12) models, with $\alpha = 0.5$ (Fig. 1; results obtained with $\alpha = 2/3$ and $\alpha = 5/6$ were qualitatively consistent). Numerical integration of Eq. 15 with $\alpha = 1$ was in good agreement with Eq. 16. For TDD, results are obtained from those calculated for Fickian diffusion, simply by rescaling the time.

Fig. 1 *a* shows the characteristic effect of anomalous subdiffusion on the fractional recovery kinetics, $f(t)$, which

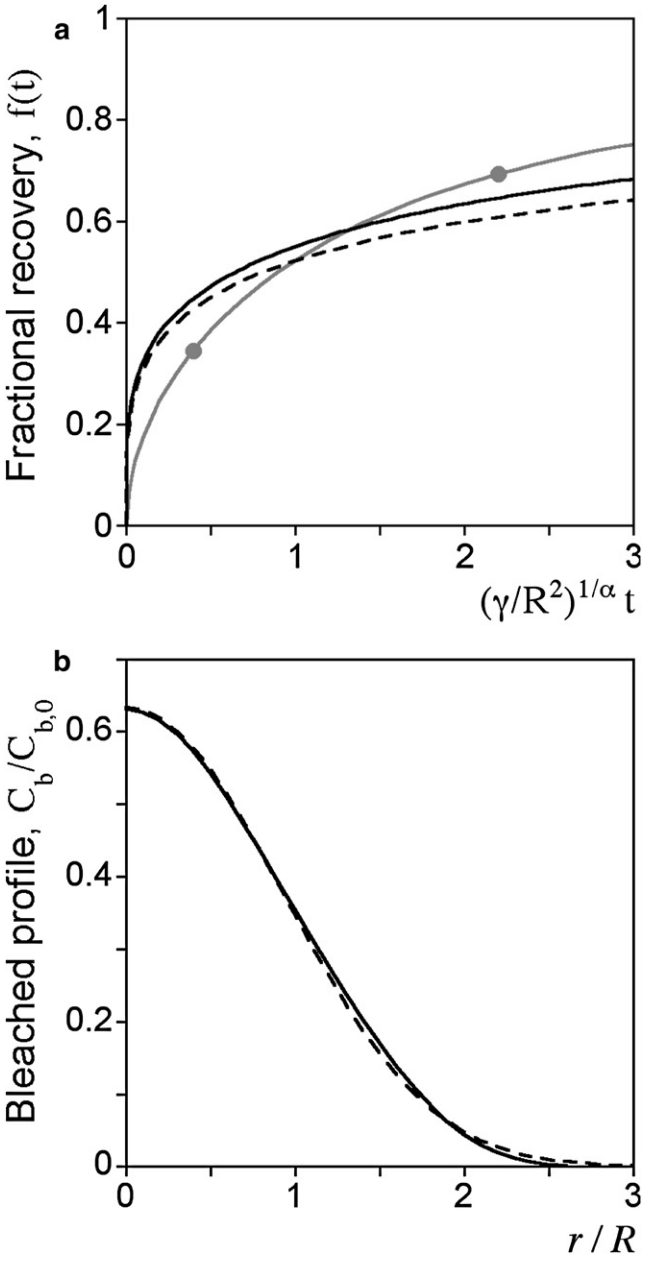

FIGURE 1 Numerical analysis of fluorescence recovery after photobleaching (FRAP) with anomalous subdiffusion. The initial bleach is assumed to be uniform and cylindrical. Gray curve with symbols, Fickian diffusion ($\alpha = 1$); solid black curve, LDD model with $\alpha = 0.5$; dashed black curve, TDD model with $\alpha = 0.5$. (*a*) Fractional fluorescence recovery, $f(t)$, calculated as a function of dimensionless time, $(\gamma/R^2)^{1/\alpha}t$, by numerical integration (Eq. 15). (*b*) Spatial concentration profiles of bleached molecules at equivalent $f(t)$, calculated by numerical integration (Eq. 14).

is already known for the TDD model (7,20). By comparison, the LDD model produces subtle yet noticeable differences for given values of γ and α; the LDD shows somewhat greater recovery at longer times. If LDD were the ''correct'' model of anomalous diffusion, would fitting the data using the well-known TDD model fail? No. By reducing the value of γ and increasing the value of α by modest amounts, the

TDD model can be made to overlap LDD-based recovery kinetics precisely. For $\alpha = 0.5$, the fit value of α using the TDD model would be ~0.54, and the fit value of γ would be ~88% of the true value (results not shown).

Whereas the spatially averaged recovery kinetics cannot reliably distinguish between the two models, how about the shape of the bleached fluorescence profile? Fig. 1 *b* shows bleached profiles for the TDD and LDD models, calculated at different times so that the fractional recovery, *f*, is equivalent ($(\gamma/R^2)^{1/\alpha}t = 1$ for TDD, 0.79 for LDD). With the profiles normalized in this way, the difference between the two models is subtle. The tails of the profiles at higher r are slightly different because of the r-dependence of the PDF, which is proportional to $\exp(-r^2)$ for TDD and proportional to $\exp(-r^{2/\alpha})$ for LDD; however, deviation of LDD behavior from fits to the TDD model would almost certainly be obscured by experimental noise. Similar results were obtained for an initial bleach with Gaussian shape (results not shown).

Rate of capture/reaction in cells: the Smoluchowski diffusion limit

In the well-known Smoluchowski problem, the steady rate of disappearance of a diffusing species caused by a perfect, spherical absorber with radius R is derived. The classical application of this calculation is to estimate bimolecular reaction rates in the diffusion-controlled limit; it has also been used to characterize the efficiency with which molecules are captured by cells (26,27). Here, the Green's function approach is used to derive a generalized bimolecular rate constant applicable to anomalous diffusion in three dimensions. This simplified approach is meant to complement Monte Carlo simulations that have explored the effects of molecular crowding, in particular on reaction kinetics (4,28–31).

The problem is cast in general terms as follows. At steady state, the concentration of the diffusing species is conserved by

$$\begin{aligned} \frac{\partial C(r,t)}{\partial t} &= -\frac{1}{r^2}\frac{\partial}{\partial r}\left(r^2 J_r\right) = 0; \\ C(R,t) &= 0; \quad C(\infty,t) = C_\infty. \end{aligned} \tag{17}$$

Defining C_{ab} as the concentration of absorbers, the rate of absorption is expressed in terms of an effective second-order rate constant, k_{eff}:

$$\begin{aligned} \text{rate} &= k_{\text{eff}} C_\infty C_{\text{ab}}; \\ k_{\text{eff}} C_\infty &= 4\pi R^2 J_R; \quad J_R = -J_r|_{r=R}. \end{aligned} \tag{18}$$

Fick's law (Eq. 2) produces the well-known result, $k_{eff} = 4\pi RD$ (where D is the sum of the two associating species' diffusivities, and conversion from molecules to moles as needed is implicit). For Fickian diffusion in one or two dimensions, there is no analog of the Smoluchowski problem, because the flux at any location vanishes with time (32).

Formulating the Smoluchowski problem in terms of the Green's function,

$$C(r) = C_\infty - J_R \int_S \left[\int_0^\infty G_3(\mathbf{r}, t|\mathbf{r}')dt \right] dS', \tag{19}$$

where the surface integral is taken over points $\mathbf{r}_S$ on the surface of the absorber (5). For the LDD model (Eq. 10), the quantity in brackets in Eq. 19, called $g_{3,ss}$, is

$$g_{3,\text{ss}}(|\mathbf{r} - \mathbf{r}'|) = \frac{\alpha\Gamma(3\alpha/2 - 1)}{8\pi\Gamma(3\alpha/2)\Lambda}(|\mathbf{r} - \mathbf{r}'|)^{-3+2/\alpha}. \tag{20}$$

As expected, Eq. 20 reveals that anomalous subdiffusion, to the extent that $\alpha \leq 2/3$, gives rise to the behavior seen for Fickian diffusion in one or two dimensions. That is, the depletion zone around the absorber would spread out to infinity, or until length scales are reached where diffusion is no longer anomalous. Since our goal is to evaluate k_{eff}, one sets $C(R) = 0$, and

$$k_{\text{eff}} = 4\pi R^2 \left[\int_S g_{3,ss}(|\mathbf{r}_S - \mathbf{r}'|)dS' \right]^{-1}. \tag{21}$$

Partial diffusion control, via the Collins-Kimball boundary condition $4\pi R^2 J_R = k_2 C(R)$, where k_2 is a second-order rate constant, is readily incorporated by substitution into Eq. 19; it gives the usual form of k_{eff} relative to the perfect absorber (large k_2) case. Noting that the distance between two points on the sphere's surface, $(R, 0)$ and (R, θ), is equal to $2^{1/2}R(1 - \cos\theta)^{1/2}$, Eq. 21 is evaluated based on concepts presented in section 10.3 of Carslaw and Jaeger (33), to obtain

$$\begin{aligned} k_{\text{eff}} &= 2\left[\int_0^\pi g_{3,\text{ss}}(2^{1/2}R(1 - \cos\theta)^{1/2})\sin\theta d\theta \right]^{-1} \\ &= 2\left[\int_{-1}^1 g_{3,\text{ss}}(2^{1/2}R(1 - z)^{1/2})dz \right]^{-1} \\ &= \frac{32(2 - \alpha)\Gamma(3\alpha/2)\pi}{4^{1/\alpha}\alpha^2\Gamma(3\alpha/2 - 1)} R^{3-2/\alpha}\Lambda, \end{aligned} \tag{22}$$

or, in terms of γ,

$$\frac{k_{\text{eff}}}{R^{3-2/\alpha}\gamma^{1/\alpha}} = \frac{8(2 - \alpha)[\Gamma(3\alpha/2)]^{1+1/\alpha}\pi}{[4\Gamma(5\alpha/2)]^{1/\alpha}\Gamma(3\alpha/2 - 1)}. \tag{23}$$

For comparison, the analogous result for TDD (Eq. 12) is found to be

$$\frac{k_{\text{eff}}}{R^{3-2/\alpha}\gamma^{1/\alpha}} = \frac{4(2 - \alpha)\pi^{3/2}}{6^{1/\alpha}\Gamma(3/2 - 1/\alpha)}. \tag{24}$$

The two expressions for the scaled rate constant as functions of α are compared in Fig. 2. As expected, both give the same values at $\alpha = 1$ and at $\alpha = 2/3$ ($k_{eff} = 0$), and, for the same value of α, the maximum percent difference between the LDD and TDD results is 47% (where α approaches the 2/3 cutoff). The linear function of α,

$$\frac{k_{\text{eff}}}{R^{3-2/\alpha}\gamma^{1/\alpha}} = 2\pi(\alpha - 2/3), \tag{25}$$

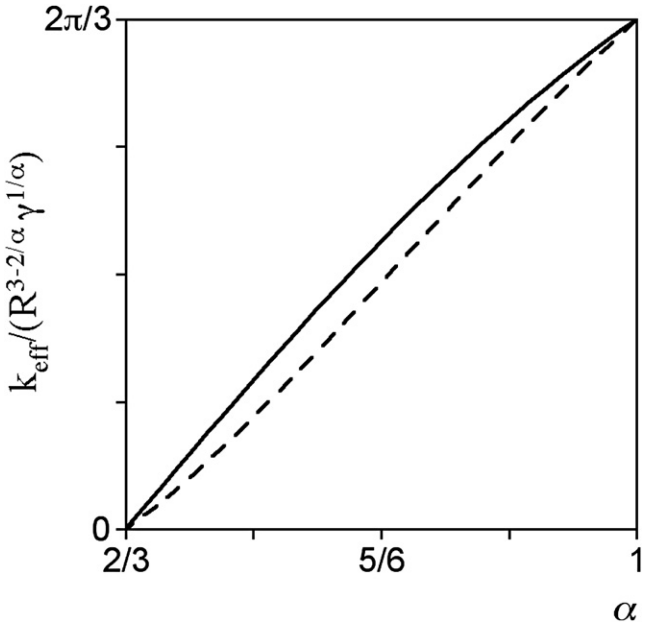

FIGURE 2 Analytical solutions for the Smoluchowski problem with anomalous subdiffusion. The effective rate constant, k_{eff}, for diffusion-limited capture by a perfectly absorbing sphere of radius R scales with $R^{3-2/\alpha}\gamma^{1/\alpha}$. The scaled effective rate constant is plotted as a function of α for the LDD (*solid curve*; Eq. 23) and TDD (*dashed curve*; Eq. 24) models.

is a reasonable compromise that might be invoked when the choice of PDF is not clear.

It is noteworthy that the appropriateness of such equations depends on whether the PDF is valid over the length scale of R. For bimolecular collisions, where R is of molecular dimensions (1–10 nm), the extrapolation of subdiffusive behavior with constant α is dubious, whereas it is expected to be more appropriate for somewhat larger spatial scales.

Spatial range of a reactive molecule

The Green's function approach may also be used to derive the spatial range of a molecule being consumed by a first-order reaction with rate constant k_1. This problem is classically associated with reactions in porous catalysts (34) and has more recently been applied to enzymatic conversions in cells (35–37) and on cell membranes (38,39); pseudo-first-order kinetics are appropriate when the enzyme is far from saturation. The result is obtained from

$$\langle |r| \rangle = 2A_n k_1 \int_0^\infty \left[\int_0^\infty p_n(r,t) r^n dr \right] e^{-k_1 t} dt. \qquad (26)$$

For the LDD model (Eq. 10), the more general dynamic length scale is

$$\langle |r| \rangle = \frac{\Gamma\left[\frac{(n+1)\alpha}{2}\right]\Gamma\left(1+\frac{\alpha}{2}\right)}{\Gamma(n\alpha/2)} \left(\frac{4\Lambda}{\alpha^2 k_1}\right)^{\alpha/2} \qquad (27)$$

or, in terms of γ,

$$\frac{\langle |r| \rangle}{\left(\gamma/k_1^\alpha\right)^{1/2}} = \frac{\Gamma\left[\frac{(n+1)\alpha}{2}\right]\Gamma\left(1+\frac{\alpha}{2}\right)}{\left\{\Gamma\left[\frac{(n+2)\alpha}{2}\right]\Gamma(n\alpha/2)\right\}^{1/2}}. \qquad (28)$$

For the TDD model (Eq. 12), the analogous result is

$$\frac{\langle |r| \rangle}{\left(\gamma/k_1^\alpha\right)^{1/2}} = \left(\frac{2}{n}\right)^{1/2} \frac{\Gamma\left(\frac{n+1}{2}\right)\Gamma\left(1+\frac{\alpha}{2}\right)}{\Gamma(n/2)}. \qquad (29)$$

Fig. 3 shows that the coefficients on the right-hand sides of Eqs. 28 and 29 are weak functions of α; for LDD, the value is ~20% higher at $\alpha = 0$ than at $\alpha = 1$ for all n, and for TDD, the value is 13% higher at $\alpha = 0$.

A different definition of the dynamic length scale is obtained by considering the steady-state flux associated with diffusing molecules that are steadily generated at one surface ($x = 0$) and consumed as they diffuse into the object ($x > 0$), which is treated as semi-infinite. If the flux into the object is defined as J_0, then the steady-state concentration profile is given by

$$C(x) = (J_0/2) \int_0^\infty p_1(x,t) e^{-k_1 t} dt. \qquad (30)$$

The factor of 1/2 renormalizes the one-dimensional PDF to account for the domain extending in the direction of $x > 0$

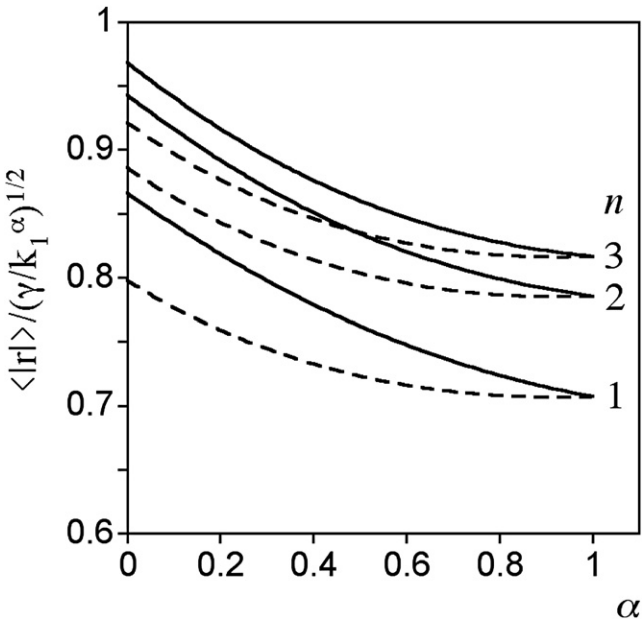

FIGURE 3 Analytical solutions for the spatial range of a molecule with finite lifetime undergoing anomalous subdiffusion. The average displacement $\langle |r| \rangle$ of a molecule consumed by first-order reaction (rate constant k_1) scales with $(\gamma/k_1^\alpha)^{1/2}$. The scaled spatial range is plotted as a function of α for the LDD (*solid curves*; Eq. 28) and TDD (*dashed curves*; Eq. 29) models, for subdiffusion in $n = 1$, 2, and 3 dimensions, as indicated.

only. Typically, the concentration at the surface is specified, in which case

$$\begin{aligned} C(0) &= C_0; \\ J_0 &= 2C_0\left[\int_0^\infty p_1(0,t)e^{-k_1 t}dt\right]^{-1}. \end{aligned} \tag{31}$$

For the LDD (Eq. 10),

$$\frac{J_0}{k_1 C_0} = \frac{\Gamma(\alpha/2)}{\Gamma(1-\alpha/2)}\left(\frac{\alpha}{2}\right)\left(\frac{4\Lambda}{\alpha^2 k_1}\right)^{\alpha/2}, \tag{32}$$

or, within 5% accuracy, for $\alpha < 1$,

$$\frac{J_0}{k_1 C_0} \approx \left(\frac{\Lambda}{\alpha^2 k_1}\right)^{\alpha/2}. \tag{33}$$

Dividing the dynamic length scale, given by either Eq. 32 or the approximate Eq. 33, by the thickness of the object gives the effectiveness factor for the reaction (34). It is noted that equating the dynamic length scale and $\langle|r|\rangle$ (Eq. 27, with $n = 1$) is exact for $\alpha = 1$ only; in general, for $\alpha < 1$, that assumption underestimates the overall reaction rate by as much as a factor of 2.

Two-state reaction-diffusion systems in cell membranes

The final example entails the potentially diffusion-limited enzymatic reactions on planar surfaces. This is a relevant problem in signal transduction, because cell surface receptors initiate intracellular pathways through recruitment of enzymes to the inner face of the plasma membrane, as explored previously ((40) and references therein). A simple but relevant case is that of the collision coupling mechanism, wherein a membrane-anchored signaling molecule cycles between two states, inactive and active. Variations of this model have been invoked, assuming Fickian diffusion, to describe the activation of heterotrimeric G-proteins (41) and small GTPases of the Ras family (42).

The catalyst for activation is a perfectly reactive disk with radius R (the encounter radius). As the activated species diffuses away from that site, it is converted back to the inactive state by a pseudo-first-order reaction with rate constant k_1. If the activation sites are sufficiently sparse, the boundary conditions governing the concentration of the inactive species, $C(r)$, are $C(R) = 0$ and $C(\infty) = C_\infty$. Integrating over the surface of the disk, the relationship at steady state between $C(r)$ and the flux at the surface, J_R, is given by

$$C(r) = C_\infty - J_R\int_S\left[\int_0^\infty G_2(\mathbf{r},t|\mathbf{r}')e^{-k_1 t}dt\right]dS'. \tag{34}$$

Setting $C(R) = 0$ for the diffusion-controlled limit,

$$\begin{aligned} \frac{J_R}{C_\infty} &= \left\{\int_S\left[\int_0^\infty G_2(\mathbf{r}_S,t|\mathbf{r}')e^{-k_1 t}dt\right]dS'\right\}^{-1} \\ &= \left\{2R\int_0^\pi\left[\int_0^\infty G_2(\mathbf{r}_S,t|\mathbf{r}_S')e^{-k_1 t}dt\right]d\theta\right\}^{-1}, \end{aligned} \tag{35}$$

with $|\mathbf{r}_S - \mathbf{r}_S'| = 2^{1/2}R(1-\cos\theta)^{1/2}$. The effective activation rate constant is related to this quantity by

$$k_{\text{eff}} = 2\pi R\left(J_R - J_R^*\right)/C_\infty. \tag{36}$$

The subtraction of the flux J_R^* adjusts the total flux to account for the fraction of the active molecules released at $r = R$ that are consumed by first-order reaction inside the disk. This quantity is calculated by finding the average concentration in the disk:

$$\begin{aligned} J_R^* &= \frac{k_1}{R}\int_0^R[C_\infty - C(r)]rdr; \\ \frac{J_R^*}{J_R} &= 2k_1\int_0^R\left\{\int_0^\pi\left[\int_0^\infty G_2(\mathbf{r},t|\mathbf{r}_S')e^{-k_1 t}dt\right]d\theta\right\}rdr, \end{aligned} \tag{37}$$

with $|\mathbf{r} - \mathbf{r}_S'| = (R^2 + r^2 - 2rR\cos\theta)^{1/2}$. When the inactivation rate is slow, a suitable approximation is to assume a constant concentration, $C(r) \approx 0$, inside the disk ($J_R^*/C_\infty \approx k_1 R/2$).

Dimensional analysis of Eqs. 35–37 shows that for both LDD and TDD models, the effective rate constant can be expressed in dimensionless form as

$$\frac{k_{\text{eff}}}{R^{2-2/\alpha}\gamma^{1/\alpha}} = f\left[k_1\left(4R^2/\gamma\right)^{1/\alpha}\right]. \tag{38}$$

The quantity in brackets is defined as the Damköhler number for first-order reaction, Da; the factor of 4 is included to facilitate comparison to the Fickian diffusion case ($\alpha = 1$, $\gamma = 4D$), which is (43)

$$\frac{k_{\text{eff}}}{\gamma} = \frac{\pi}{2}\frac{Da^{1/2}K_1\left(Da^{1/2}\right)}{K_0\left(Da^{1/2}\right)}, \tag{39}$$

where $K_0(x)$ and $K_1(x)$ are modified Bessel functions of the second kind (19). As noted for the Smoluchowski problem in three dimensions, partial diffusion control may be accommodated in the usual way once the diffusion-limited rate constant is found.

Equations 35 and 37 were integrated numerically for the LDD and TDD models. For $\alpha = 1$, the numerically computed values of k_{eff} are in very close agreement with the exact solution, Eq. 39. This validation step shows the importance of the flux correction in Eqs. 36 and 37, at least for the higher values of Da; were the correction omitted, the numerically computed value of k_{eff} for $Da = 1$ would be 33% too high.

Fig. 4 shows that the two models produce similar relationships of the form prescribed by Eq. 38. In the relevant case of $Da << 1$, for which the spatial range of activated molecules is much larger than the encounter radius, the effective rate constant for Fickian diffusion (Eq. 39) is insensitive to the value of Da. By comparison, the effective rate constant for subdiffusion exhibits a more sensitive dependence on the inactivation rate constant; by inspection of Fig. 4, the dependence scales roughly as $k_{\text{eff}} \propto k_1^{1-\alpha}$. This is consistent with scaling analysis of the steady-state reaction-diffusion problem,

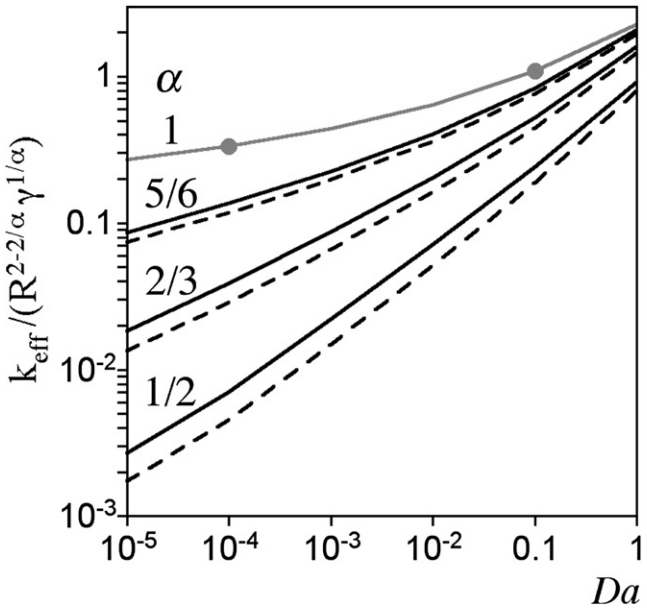

FIGURE 4 Numerical analysis of diffusion-controlled reactions on planar surfaces with anomalous subdiffusion. The effective rate constant, k_{eff}, for activation of signaling molecules by a perfectly reactive disk of radius R, subject to inactivation by first-order reaction (rate constant k_1), scales with $R^{2-2/\alpha}\gamma^{1/\alpha}$ and depends also on the Damköhler number for the inactivation reaction, $Da = k_1(4R^2/\gamma)^{1/\alpha}$. The scaled activation rate constant is plotted as a function of Da for Fickian diffusion ($\alpha = 1$; *gray curve with symbols*) and the LDD (*solid curves*) and TDD (*dashed curves*) models for the selected values of α indicated. See the text for numerical details.

incorporating the previous result for the dynamic length scale (Eqs. 28 and 29):

$$-\frac{1}{r}\frac{\partial}{\partial r}(rJ_r) = k_1C(r); \quad \frac{RJ_R}{\langle|r|\rangle^2} \sim k_1C_\infty; \qquad k_{\text{eff}} \sim k_1\langle|r|\rangle^2 \sim \gamma k_1^{1-\alpha}. \tag{40}$$

Incidentally, the average density of active molecules scales roughly as $k_{\text{eff}}/k_1 \propto k_1^{-\alpha}$. Thus, for subdiffusion, the average density is less sensitive to the lifetime of the activated state.

CONCLUSIONS

The Green's function approach was used to solve problems with anomalous diffusion of reactants. In each case, two conceptually distinct models that recapitulate the time dependence of the MSD as prescribed by Eq. 3 gave qualitatively similar results. What this suggests is that the results are determined largely by the scaling of diffusion length relative to time, intrinsic to MSD(t). It also shows that a good fit to a particular model, for example, time-dependent diffusion, does not constitute credible evidence for that particular world view of what barriers to diffusion are being imposed.

By altering the relative scaling of length and time, anomalous subdiffusion influences diffusion-limited reactions in interesting ways. For absorption in solution, subdiffusion effectively reduces the dimensionality, which might be relevant for enhancing the likelihood of capture (44). For reversible activation/deactivation mechanisms in cell membranes, subdiffusion increases the sensitivity of the activation rate constant to the lifetime of the activated state in a way that makes the average density of activated molecules less sensitive to their lifetime.

This work was partially supported by an award to J.M.H. from the Camille and Henry Dreyfus Foundation (TC-05-022).

REFERENCES

1. Bray, D. 1998. Signaling complexes: biophysical constraints on intracellular communication. *Annu. Rev. Biophys. Biomol. Struct.* 27:59–75.
2. Sheetz, M. P. 1993. Glycoprotein motility and dynamic domains in fluid plasma membranes. *Annu. Rev. Biophys. Biomol. Struct.* 22: 417–431.
3. Kusumi, A., C. Nakada, K. Ritchie, K. Murase, K. Suzuki, et al. 2005. Paradigm shift of the plasma membrane concept from the two-dimensional continuum fluid to the partitioned fluid: High-speed single-molecule tracking of membrane molecules. *Annu. Rev. Biophys. Biomol. Struct.* 34:351–378.
4. Grima, R., and S. Schnell. 2006. A systematic investigation of the rate laws valid in intracellular environments. *Biophys. Chem.* 124:1–10.
5. Deen, W. M. 1998. Analysis of Transport Phenomena. Oxford University Press, New York.
6. Agutter, P. S., P. C. Malone, and D. N. Wheatley. 1995. Intracellular transport mechanisms: a critique of diffusion theory. *J. Theor. Biol.* 176:261–272.
7. Feder, T. J., I. Brust-Mascher, J. P. Slattery, B. Baird, and W. W. Webb. 1996. Constrained diffusion or immobile fraction on cell surfaces: a new interpretation. *Biophys. J.* 70:2767–2773.
8. Schwille, P., J. Korlach, and W. W. Webb. 1999. Fluorescence correlation spectroscopy with single-molecule sensitivity on cell and model membranes. *Cytometry.* 36:176–182.
9. Weiss, M., M. Elsner, F. Kartberg, and T. Nilsson. 2004. Anomalous subdiffusion is a measure for cytoplasmic crowding in living cells. *Biophys. J.* 87:3518–3524.
10. Dix, J. A., and A. S. Verkman. 2008. Crowding effects on diffusion in solutions and cells. *Annu. Rev. Biophys.* 37:247–263.
11. Saxton, M. J., and K. Jacobson. 1997. Single-particle tracking: applications to membrane dynamics. *Annu. Rev. Biophys. Biomol. Struct.* 26:373–399.
12. Nicolau, D. V., J. F. Hancock, and K. Burrage. 2007. Sources of anomalous diffusion on cell membranes: a Monte Carlo study. *Biophys. J.* 92:1975–1987.
13. Wu, J., and K. M. Berland. 2008. Propagators and time-dependent diffusion coefficients for anomalous diffusion. *Biophys. J.* 95:2049–2052.
14. del-Castillo-Negrete, D., B. A. Carreras, and V. E. Lynch. 2005. Nondiffusive transport in plasma turbulence: a fractional diffusion approach. *Phys. Rev. Lett.* 94:065003.
15. Barkai, E., R. Metzler, and J. Klafter. 2000. From continuous time random walks to the fractional Fokker-Planck equation. *Phys. Rev. E.* 61:132–138.
16. Saxton, M. J. 1994. Anomalous diffusion due to obstacles: a Monte Carlo study. *Biophys. J.* 66:394–401.
17. Saxton, M. J. 1996. Anomalous diffusion due to binding: a Monte Carlo study. *Biophys. J.* 70:1250–1262.
18. O'Shaughnessy, B., and I. Procaccia. 1985. Analytical solutions for diffusion on fractal objects. *Phys. Rev. Lett.* 54:455–458.
19. Abramowitz, M., and I. A. Stegun. 1974. Handbook of Mathematical Functions, With Formulas, Graphs. Mathematical Tables, Dover, New York.

20. Saxton, M. J. 2001. Anomalous subdiffusion in fluorescence photobleaching recovery: a Monte Carlo study. *Biophys. J.* 81:2226–2240.

21. Axelrod, D., D. E. Koppel, J. Schlessinger, E. Elson, and W. W. Webb. 1976. Mobility measurement by analysis of fluorescence photobleaching recovery kinetics. *Biophys. J.* 16:1055–1069.

22. Lippincott-Schwartz, J., E. Snapp, and A. Kenworthy. 2001. Studying protein dynamics in living cells. *Nat. Rev. Mol. Cell Biol.* 2:444–456.

23. Periasamy, N., and A. S. Verkman. 1998. Analysis of fluorophore diffusion by continuous distributions of diffusion coefficients: application to photobleaching measurements of multicomponent and anomalous diffusion. *Biophys. J.* 75:557–567.

24. Lubelski, A., and J. Klafter. 2008. Fluorescence recovery after photobleaching: the case of anomalous diffusion. *Biophys. J.* 94:4646–4653.

25. Soumpasis, D. M. 1983. Theoretical analysis of fluorescence photobleaching recovery experiments. *Biophys. J.* 41:95–97.

26. Berg, H. C., and E. M. Purcell. 1977. Physics of chemoreception. *Biophys. J.* 20:193–219.

27. Coppey, M., A. M. Berezhkovskii, S. C. Sealfon, and S. Y. Shvartsman. 2007. Time and length scales of autocrine signals in three dimensions. *Biophys. J.* 93:1917–1922.

28. Saxton, M. J. 2002. Chemically limited reactions on a percolation cluster. *J. Chem. Phys.* 116:203–208.

29. Berry, H. 2002. Monte Carlo simulations of enzyme reactions in two dimensions: fractal kinetics and spatial segregation. *Biophys. J.* 83:1891–1901.

30. Minton, A. P. 2006. How can biochemical reactions within cells differ from those in test tubes? *J. Cell Sci.* 119:2863–2869.

31. Ridgway, D., G. Broderick, A. Lopez-Campistrous, M. Ru'aini, P. Winter, et al. 2008. Coarse-grained molecular simulation of diffusion and reaction kinetics in a crowded virtual cytoplasm. *Biophys. J.* 94: 3748–3759.

32. Torney, D. C., and H. M. McConnell. 1983. Diffusion-limited reaction rate theory for two-dimensional systems. *Proc. R. Soc. Lond. A.* 387: 147–170.

33. Carslaw, H. S., and J. C. Jaeger. 1959. Conduction of Heat in Solids. Oxford University Press, New York.

34. Aris, R. 1957. On shape factors for irregular particles. I. The steady state problem. Diffusion and reaction. *Chem. Eng. Sci.* 6:262–268.

35. Brown, G. C., and B. N. Kholodenko. 1999. Spatial gradients of cellular phospho-proteins. *FEBS Lett.* 457:452–454.

36. Meyers, J., J. Craig, and D. J. Odde. 2006. Potential for control of signaling pathways via cell size and shape. *Curr. Biol.* 16:1685–1693.

37. Haugh, J. M. 2007. Membrane-binding/modification model of signaling protein activation and analysis of its control by cell morphology. *Biophys. J.* 92:L93–L95.

38. Postma, M., and P. J. M. van Haastert. 2001. A diffusion-translocation model for gradient sensing by chemotactic cells. *Biophys. J.* 81:1314–1323.

39. Haugh, J. M., and I. C. Schneider. 2006. Effectiveness factor for spatial gradient sensing in living cells. *Chem. Eng. Sci.* 61:5603–5611.

40. Monine, M. I., and J. M. Haugh. 2008. Signal transduction at point-blank range: analysis of a spatial coupling mechanism for pathway crosstalk. *Biophys. J.* 95:2172–2182.

41. Shea, L. D., G. M. Omann, and J. J. Linderman. 1997. Calculation of diffusion-limited kinetics for the reactions in collision coupling and receptor cross-linking. *Biophys. J.* 73:2949–2959.

42. Monine, M. I., and J. M. Haugh. 2005. Reactions on cell membranes: comparison of continuum theory and Brownian dynamics simulations. *J. Chem. Phys.* 123:074908.

43. Freeman, D. L., and J. D. Doll. 1983. The influence of diffusion on surface reaction kinetics. *J. Chem. Phys.* 78:6002–6009.

44. Adam, G., and M. Delbrück. 1968. Reduction of dimensionality in biological diffusion processes. *In* Structural Chemistry and Molecular Biology. A. Rich, and N. Davidson, editors. W. H. Freeman and Co., San Francisco. 198–215.